lubricants

MDPI

Article

Comparative Study of Tribological Properties of Modified and Non-modified Graphene-Oil Nanofluids under Heated and Non-heated Conditions

Kean Pin Ng, Kia Wai Liew * and Elaine Lim

SIG: Machine Design and Tribology, Centre for Advanced Mechanical & Green Technology (CAMGT), Faculty of Engineering & Technology, Multimedia University, Melaka 75450, Malaysia
* Correspondence: kwliew@mmu.edu.my

Abstract: With the aim of achieving more effective friction and wear reduction in sliding bearing applications, surface-modified graphene, which exhibits better dispersion stability than non-modified graphene, was synthesized and applied in this study using various graphene allotropes, including graphene nanoplatelets (GNP), multiwalled carbon nanotubes (MWCNT) and nanostructured graphite (NSG). Friction and wear tests of each type of graphene allotrope under modified and non-modified conditions were studied using a pin-on-ring tribo tester. In addition, the dynamic viscosity of each synthesized nanofluid sample was measured using a falling-ball viscometer. A series of modified graphene-oil nanofluids and non-modified graphene-oil nanofluids were prepared and heated before their friction and wear performance was investigated at room temperature. Friction and wear behavior, as well as the dynamic viscosity of the heated nanofluids vary insignificantly when compared to those of the non-heated nanofluids. The results showed that the best friction and wear reduction was achieved by modified GNP with friction and wear reduction of 60.5% and 99.4%, respectively.

Keywords: graphene-oil nanofluids; heated and non-heated; tribological properties; graphene surface modification

Citation: Ng, K.P.; Liew, K.W.; Lim, E. Comparative Study of Tribological Properties of Modified and Non-modified Graphene-Oil Nanofluids under Heated and Non-heated Conditions. *Lubricants* **2022**, *10*, 288. https://doi.org/10.3390/lubricants10110288

Received: 17 September 2022
Accepted: 25 October 2022
Published: 31 October 2022

1. Introduction

Journal bearings are widely used in various types of mechanical systems, such as motors, wind turbine gearboxes and propeller shafts, especially in mechanisms with rotating shafts [1]. The presence of friction and wear within a journal bearing must be studied to ensure minimal friction and wear for better performance and longer bearing life [2,3]. For instance, minimum friction and wear of journal bearings in wind turbine gearboxes are essential to ensure maximum efficiency of the power to be delivered [4–6] and also to minimize the maintenance cost of repairing or replacing defective bearings of wind turbine gearboxes due to excessive friction and wear [7]. In order to minimize the friction and wear of journal bearings, numerous studies have been conducted in the past applying various types of advanced nano-lubrication concepts [8–10]. Among the studies conducted, graphene is found to be able to reduce friction and wear between two sliding surfaces effectively due to their unique self-lubricating tribo-film, whether under dry solid lubricating conditions [11] or in the form of liquid nano-lubricants [12,13]. When the lubricating surfaces slide over each other, the graphene layers can be sheared off easily and distributed over the lubricating surfaces forming the unique self-lubricating tribo-film owing to the weak Van der Waals force between the graphene layers [14,15]. Apart from that, graphene nanoparticles also perform a mending mechanism [16] by filling up the asperities gaps between lubricating surfaces. Furthermore, the graphene nanoparticles can also act as tiny ball bearings [17] which aids the sliding actions between two surfaces, lowering the friction coefficient trend.

In the application of journal bearing, liquid lubricating oil is used as a lubricating medium to achieve the condition of hydrodynamic lubrication [18]. Therefore, the dispersion stability of graphene in the base oil fluid is crucial to ensure the proper distribution of graphene for better friction and wear reduction [19,20]. However, not all graphene is suitable to be dispersed in base oil fluid to synthesize a stably dispersed graphene-oil nanofluid. Therefore, various approaches, including the addition of surfactant [21,22] and graphene surface modification processes [23], have been introduced in previous studies to improve the dispersion stability of graphene in base oil fluid.

The depletion of natural mineral resources is alarming and worries society because most commercial lubricating oils are made of petroleum-based mineral oil [24,25]. A new revolution of lubricating oil promoting the concept of eco-friendly and green tribology needs to be introduced. In this study, the method of lubrication with biodegradable vegetable oil is implemented. It is expected that using vegetable oil as the base oil for lubricating the journal bearings of the offshore wind turbine will help to minimize the problem of marine pollution because the oils are easily biodegradable and non-toxic.

One of the main functions of lubricating oil is to remove unwanted heat from mechanical systems [26] by absorbing the heat generated by the sliding movements between the shaft and the bearing housing, resulting in an increase in oil temperature. Studies on the thermophysical properties of nanofluids have also been conducted in the past to investigate the heat transfer performance of nanofluids compared to the normal base fluid [27–29]. It is necessary to ensure that the lubricating oil can operate efficiently at different operating temperatures. Hence, the effects of temperature on the thermophysical properties of graphene-oil nanofluids are investigated.

It is well known that multilayer graphene allotropes provide better friction and wear reduction [30,31]. In this research work, three types of most commonly found multilayer graphene allotropes, namely graphene nanoplatelets (GNP), multiwalled carbon nanotubes (MWCNT) and nanostructured graphite (NSG), are used in the formation of graphene-oil nanofluids to investigate the effects of different types of graphene nanoparticles on the tribological performance of the lubricating base fluid. In addition, the dynamic viscosity and tribological properties of the heated graphene-oil nanofluids are also investigated in this work. In short, the friction and wear performance of synthesized graphene-oil nanofluids using biodegradable vegetable oil with both unmodified and surface-modified graphene is investigated. In order to study the effects of frequent temperature cycling in a real application, the tribological performance of non-heated (fresh) and heated graphene-oil nanofluids is also investigated in this work.

2. Experimental Works

2.1. Tribo Specimens Preparation

Aluminum alloy 5083 (AL-5083) was selected as the pin specimen material to be used in this research work due to its excellent corrosive resistivity [32], which can closely simulate the journal bearings applications around marine environments such as wind turbines, propeller shafts of a ship and even a submarine. Moreover, aluminum alloy is widely applied as a bearing material due to its excellent friction performance when compared with other bearing materials such as white metal and bronze [33]. Table 1 shows the mechanical properties and chemical composition of AL-5083. Cylindrical pin specimens with a diameter of 5 mm and length of 20 mm were fabricated from AL-5083 rod. The arithmetic surface roughness, R_a of pin specimens, was controlled at 0.275 μm.

On the other hand, stainless steel 304 (SS-304) was selected as a counter ring material due to its strong mechanical properties [34,35], and it is commonly used as transmission shaft material in marine environments [36,37]. Counter rings with an inner diameter of 9 mm, an outer diameter of 22 mm and a thickness of 10 mm were machined from SS-304 rods using a CNC turning machine. Meanwhile, the R_a for all counter ring was controlled at 0.300 μm. The chemical composition and mechanical properties of SS-304 are shown in Table 2. Figure 1 shows the fabricated AL-5083 pin specimens and SS-304 counter ring.

Table 1. Chemical composition and mechanical properties of AL-5083.

Element	Compositions (wt%)
Si	0.10
Fe	0.16
Cu	0.02
Mn	0.57
Mg	4.15
Cr	0.11
Zn	0.02
Al	94.87
Mechanical Properties	
Tensile Strength	277 MPa
Yield Strength	130 MPa
Elongation Rate	13%

Table 2. Chemical composition and mechanical properties of SS-304.

Element	Compositions (wt%)
C	0.018
Mn	1.58
Si	0.28
S	0.025
P	0.035
Cr	18.14
Ni	8.07
Cu	0.61
Mo	0.31
Co	0.18
N	0.085
Fe	70.067
Mechanical Properties	
Tensile Strength	622 MPa
Yield Strength	584 MPa

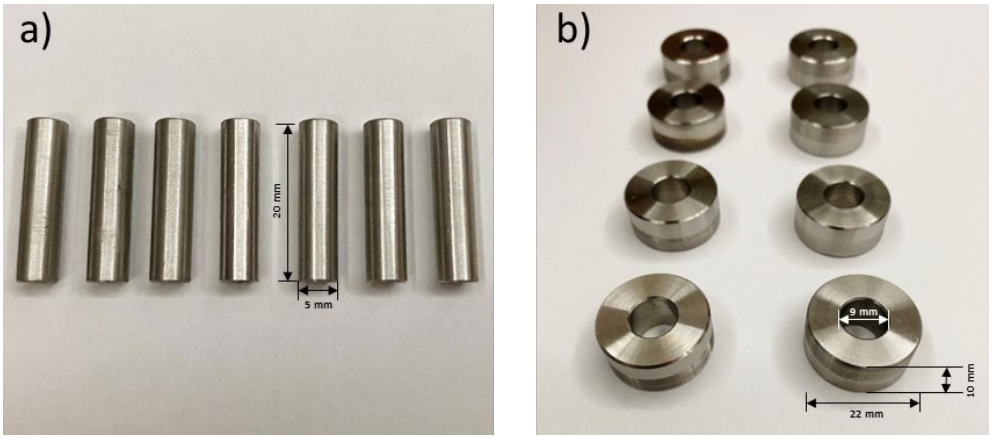

Figure 1. Photograph of (**a**) AL-5083 pin specimens and (**b**) SS-304 counter rings.

2.2. Modified and Non-modified Graphene-Oil Nanofluids Samples Preparation

Three types of multilayer graphene allotropes, namely, graphene nanoplatelets (GNP), multiwalled carbon nanotubes (MWCNT) and nanostructured graphite (NSG), were used to synthesize three types of graphene-oil nanofluids at 0.04 wt%. To improve the dispersion stability of graphene in oil, the graphene surface was modified using sodium dodecyl

sulfate (SDS) and oleic acid (OA) in this work. The modification of graphene started by mixing graphene into an SDS solution. OA was then added to the sonicated mixture of SDS and graphene solution, and another round of sonication was performed. The final mixture of the graphene–SDS-OA solution was then heated in a furnace at 180 °C for 4 h until it was completely dried out and only modified graphene powders remained.

High oleic palm oil-based methyl ester (high oleic POME) was selected as the base oil for the synthesis of graphene-oil nanofluids throughout the research because the high oleic acid content improves the oxidative properties of the base oil when used at high operating temperatures [38]. Both non-modified graphene and modified graphene were separately added to high oleic POME and sonicated with a probe sonicator, Fisher Scientific, Model: FB 705, as shown in Figure 2, for two hours to synthesize non-modified graphene-oil nanofluids and modified graphene-oil nanofluids. The synthesized GNP-oil nanofluid is referred to as GNON, while the modified GNP-oil nanofluid is referred to as mGNON in the following. MWCNT-oil nanofluid is referred to as MWON, while modified MWCNT-oil nanofluid is referred to as mMWON hereafter. NSG-oil nanofluid is referred to as NSON, while modified NSG-oil nanofluid is referred to as mNSON in the following.

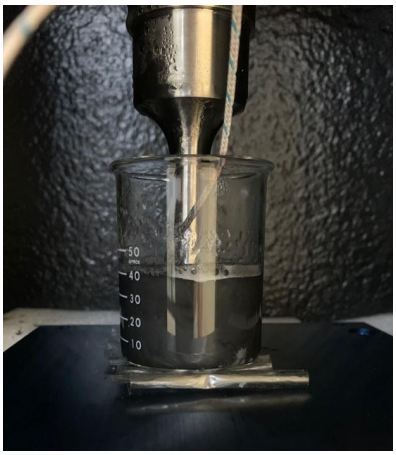

Figure 2. Sonication process of a graphene-oil nanofluid sample with a probe sonicator, Fisher Scientific, Model: FB 705.

2.3. Heating of Non-modified Graphene-Oil Nanofluids and Modified Graphene-Oil Nanofluids

Each synthesized nanofluid sample was placed in a beaker and heated with a hot plate, Faithful, model: SH-II-4C. The nanofluid in the beaker was heated from 30 °C to 85 °C in 5 °C steps, and each temperature interval was kept constant for five minutes. The heating process of the nanofluids was carried out up to 85 °C to simulate the real operating temperature of journal bearings in wind turbine gearboxes [33]. The nanofluids were then cooled naturally to room temperature. The non-heated nanofluid will be termed as "fresh" (F) in the following, while the heated and then cooled to room temperature will be referred to as "heated" (H).

2.4. Friction and Wear Test

A pin-on-ring (POR) tribo tester was used to conduct friction and wear tests in this research work via standard ASTM G-77 to simulate the real-life counter-formal contact [39] between the journal-bearing housing and transmission shaft. A schematic diagram of the POR tribo tester is shown in Figure 3. A stationary AL-5083 cylindrical pin was inserted into the specimen adaptor and tested against a rotating SS-304 counter ring, which was partially immersed into the oil container. As the counter ring started to revolve in a clockwise direction, it tended to pick up the graphene-oil nanofluids in the container and provide lubrication to the pin and ring contact surfaces. All sliding tests under boundary lubrication conditions were carried out at an ambient temperature and humidity environment with constant speed and a normal load of 1.36 m/s and 44.15 N, respectively. Modified and non-

modified graphene-oil nanofluids subjected to heated and non-heated (fresh) conditions were used as lubricating oil in sliding tests. Prior to the sliding test, both pins and counter rings were cleaned using acetone.

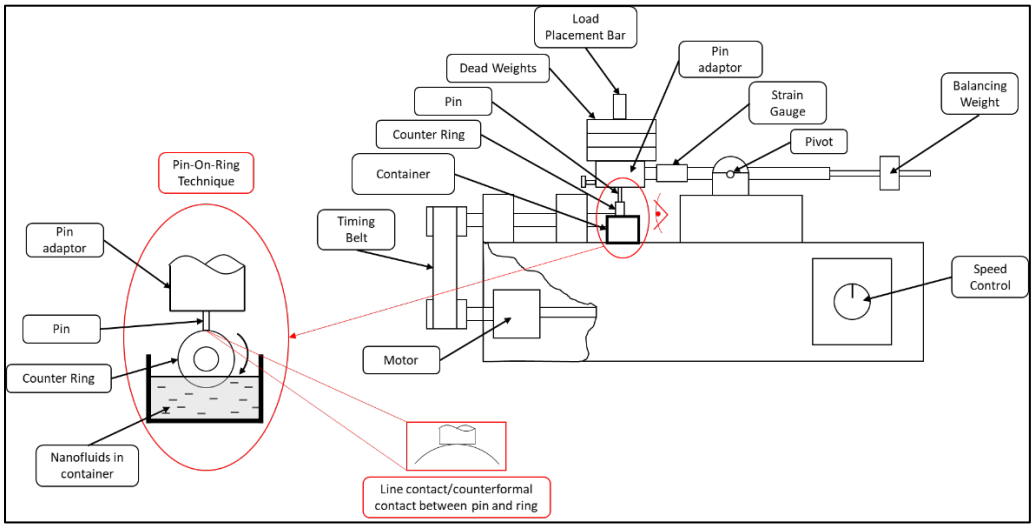

Figure 3. Schematic diagram of pin-on-ring tribo tester.

The magnitude of the tangential force F_T (N) on the sliding surface was measured with a pre-calibrated strain gauge mounted on the load level holding the pin specimen. The coefficient of friction (*CoF*) for the contact pair lubricated with different graphene-oil nanofluid samples was calculated using the ratio between the tangential force F_T (N) and the applied normal load F_N (N).

The weight loss of each pin specimen was determined by measuring the difference in weight after completion of the friction test using 0.1 mg electronic balance, SHIMADZU, Model: AW-220 (Shimadzu, Kyoto, Japan). The tribological performance of modified and non-modified graphene-oil nanofluids exposed to heated and non-heated conditions was compared. The worn surfaces of pin specimens were examined by a metallurgical microscope, Meiji, Model: MT7100 (Meiji Techno, San Jose, CA, USA).

2.5. Thermophysical Test—Dynamic Viscosity Measurement

The viscosity of the synthesized graphene-oil nanofluids was measured using a falling ball viscometer, HÖPPLER®, Model: KF 3.2, (Rheotest, Ottendorf-Okrilla, Germany), in the temperature range from 30 °C to 80 °C corresponding to the usual operating temperature of journal bearings in wind turbines [33]. The temperature range was measured and controlled using a water bath, Julabo®, Model: TW-12 (Julabo, PA, USA). Both the viscosity of non-heated (fresh) and heated graphene-oil nanofluids under non-modified and modified conditions were measured and compared.

3. Results and Discussions

3.1. Dispersion Stability

The dispersion stability of graphene-oil nanofluids is determined by observing how long it takes to observe the deposition of graphene in the sample bottles. In Figure 4, by comparing the fresh non-modified graphene-oil nanofluids, it was found that the worst dispersion stability was shown by F-MWON, where the deposition was already observed within an hour after the sonication process due to the tubular structural entanglements of the MWCNTs in the oil, which formed larger bulk clumps, as shown in the micrograph in Figure 5c. Due to the smaller nanoparticle size of NSG compared to GNP, as shown in the microscopic images in Figure 5a,b, respectively, F-NSON was observed to have better dispersion stability than F-GNON, with half of F-NSON still in black intensity, while F-GNON was already pale-gray in color on Day-7.

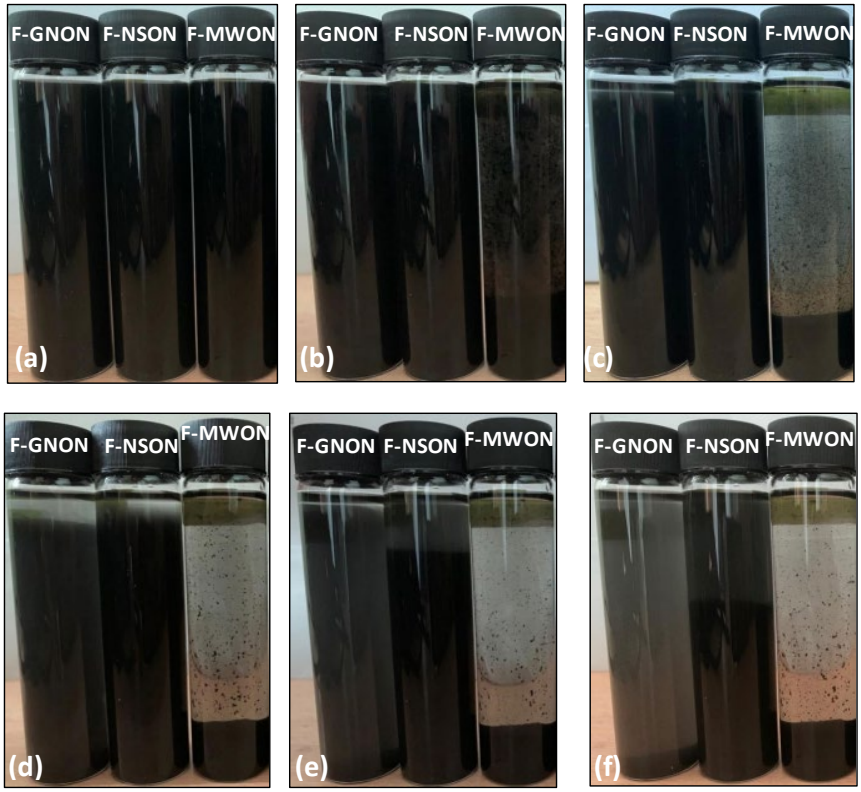

Figure 4. Dispersion stability test of fresh graphene-oil nanofluids after (**a**) completion of sonication, (**b**) one hour, (**c**) day-1, (**d**) day-3, (**e**) day-5 and (**f**) day-7 (arrangement from left: F-GNON, F-NSON and F-MWON) (Notes: F = fresh; H = heated) [40].

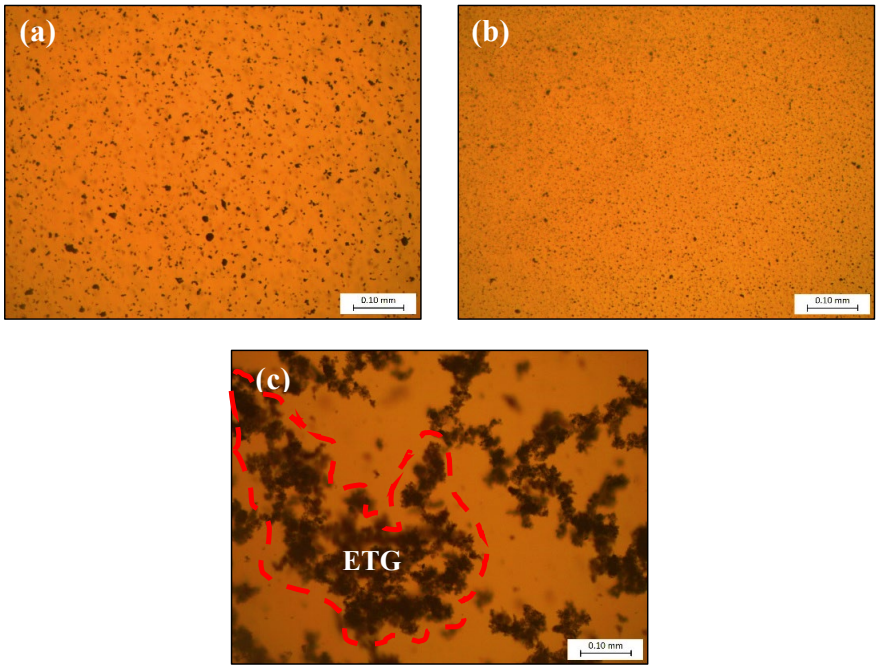

Figure 5. Micrographs of (**a**) F-GNON, (**b**) F-NSON and (**c**) F-MWON under 10× magnification (Notes: ETG = entanglement; F = fresh; H = heated).

For the fresh modified graphene-oil nanofluids (F-mGNON, F-mNSON and F-mMWON), it was observed that the dispersion stability improved significantly compared to the non-modified graphene-oil nanofluids, with the nanofluids still showing a completely dark-black

intensity after 60 days, as shown in Figure 6. Figure 7 shows the microscopic images of fresh modified graphene-oil nanofluids under 10× magnification. The dispersion stability of modified graphene in high oleic POME has greatly improved, mainly due to the increase in hydrophobicity of graphene itself after it was surface modified with sodium dodecyl sulfate (SDS) and oleic acid (OA). Due to the mixing of SDS and graphene during the first modification step, clumps of SDS adhered to the graphene surface [23], leaving the sodium ion (Na^+) exposed on the outer graphene surface. Subsequent mixing of OA into the graphene–SDS solution leads to the association of the OH^- group of OA with the Na^+ ion of the SDS compound, exposing the long hydrophobic carbon chain on the graphene surface, as illustrated in Figure 8.

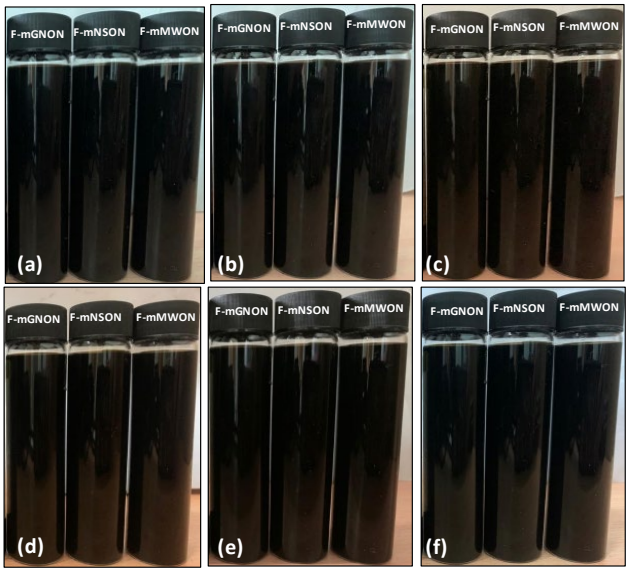

Figure 6. Dispersion stability test of fresh modified graphene-oil nanofluids after (**a**) completion of sonication, (**b**) day-1, (**c**) day-10, (**d**) day-20, (**e**) day-40 and (**f**) day-60 (arrangement from left: F-mGNON, F-mNSON and F-mMWON) (Notes: F = fresh; H = heated).

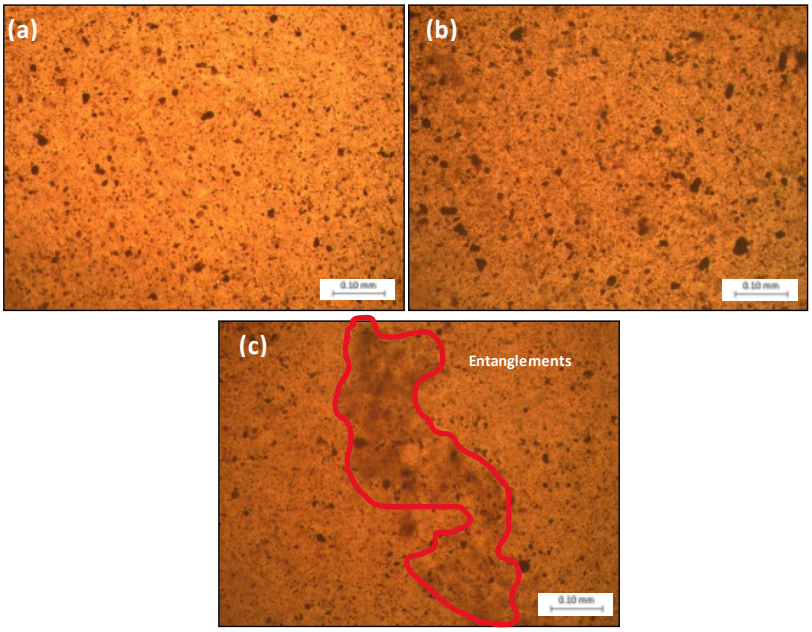

Figure 7. Micrographs of (**a**) F-mGNON, (**b**) F-mNSON and (**c**) F-mMWON under 10× magnification (Notes: F = fresh; H = heated).

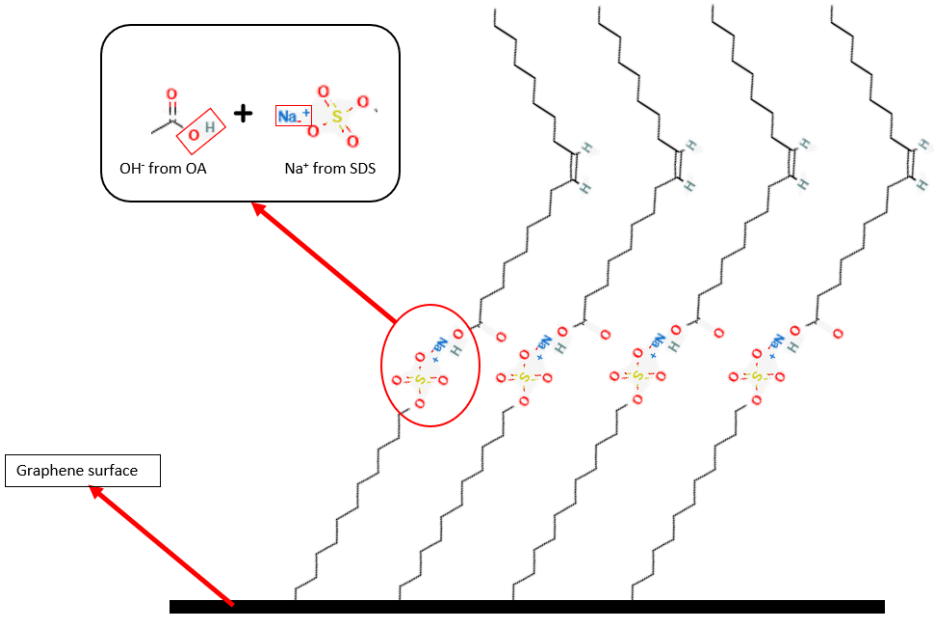

Figure 8. Reaction between sodium dodecyl sulfate (SDS) and oleic acid (OA), which adheres to the graphene surface and exposes the long hydrophobic carbon chain on the graphene surface to increase the hydrophobicity of graphene.

On the other hand, it was observed that the heated unmodified and heated modified graphene-oil nanofluids exhibited exactly the same dispersion stability as the fresh ones, as shown in Figure 9.

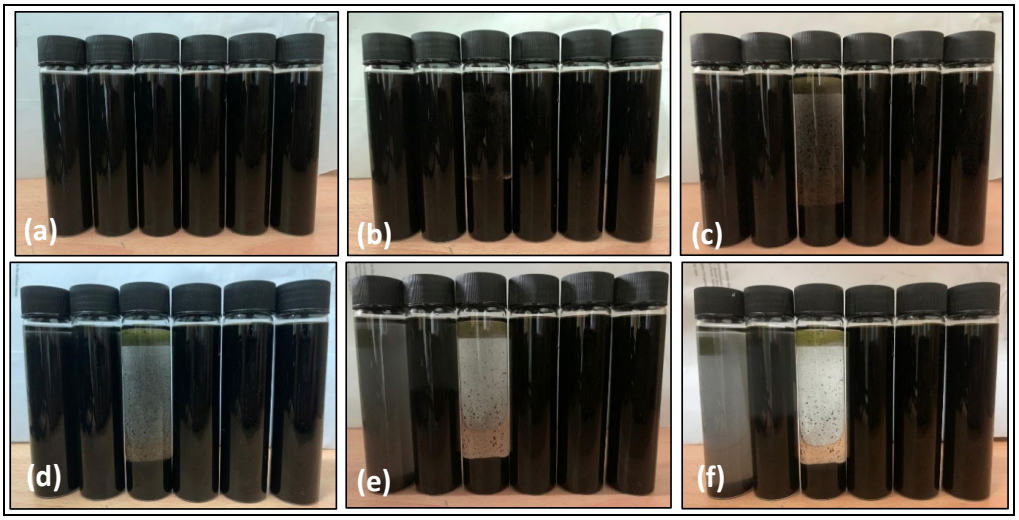

Figure 9. Dispersion stability test of heated graphene oil nanofluids and heated modified graphene-oil nanofluids after (**a**) completion of sonication, (**b**) one hour, (**c**) day-1, (**d**) day-3, (**e**) day-5 and (**f**) day-7 (arrangement from left: H-GNON, H-NSON, H-MWON, H-mGNON, H-mNSON and H-mMWON) (Notes: F = fresh; H = heated).

3.2. Dynamic Viscosity

All unmodified graphene-oil nanofluids have slightly higher dynamic viscosity than pure high oleic POME and show a decreasing tendency when the temperature gradually increases from 30 °C to 80 °C, as shown in Figure 10, mainly due to the thermal energy absorbed by the base oil molecules. This resulted in the base oil molecules having sufficient energy to overcome the intermolecular bonding between the molecules [41].

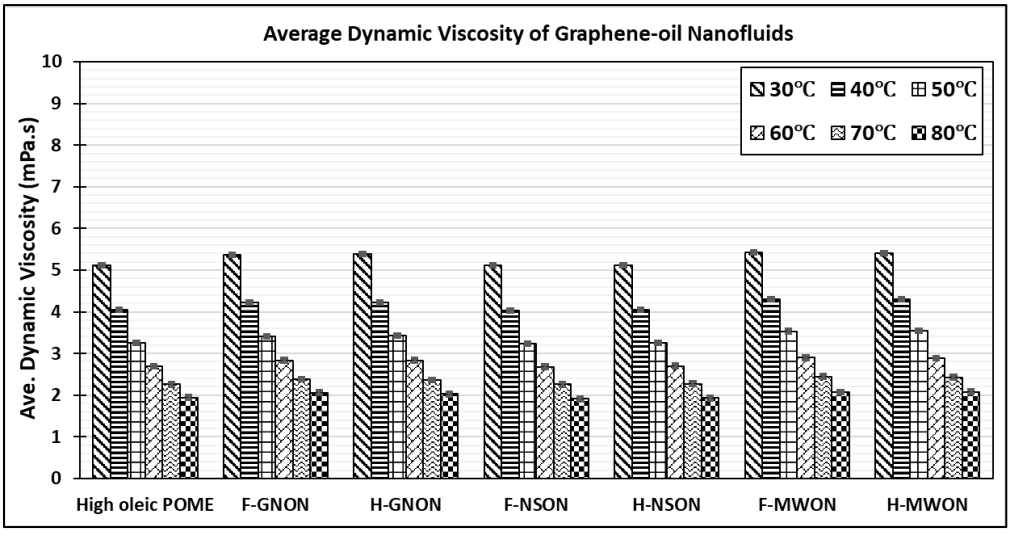

Figure 10. The average dynamic viscosity of non-heated (fresh) and heated non-modified graphene-oil nanofluids exposed to different temperatures ranges from 30 °C to 80 °C (Notes: F = fresh; H = heated).

The dynamic viscosity of non-modified graphene-oil nanofluids is closely related to the concept of solid fraction hindering the motions of liquid molecules [42], with MWON having the highest dynamic viscosity due to the fractured fragments of MWCNT formed [43] during sonication (largest solid fraction), followed by GNON and finally NSON, where GNP is slightly larger than NSG (solid fraction in GNON larger than NSON) as evidenced in Figure 5a,b. Figure 11 shows the presence of broken MWCNT fragments after the sonication process, leading to a significant increase in the solid fraction in MWON. When compared with heated non-modified graphene-oil nanofluids, no significant changes in dynamic viscosity were observed, as shown in Figure 10.

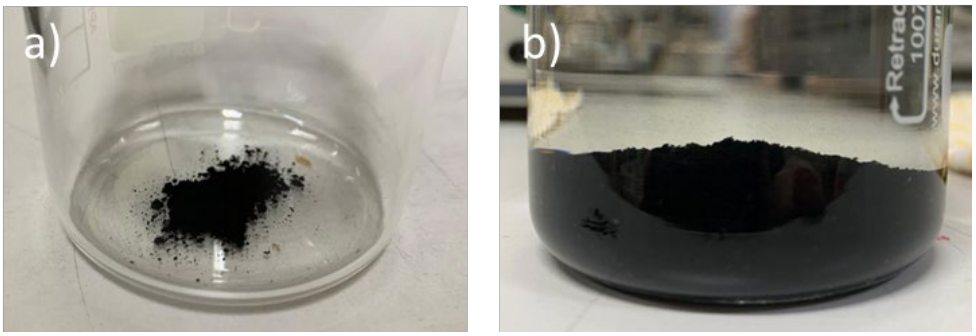

Figure 11. Equal amount of MWCNTs as solid fraction (**a**) before and (**b**) after sonication at complete sedimentation.

Meanwhile, all modified graphene-oil nanofluids show a significant increase in dynamic viscosity compared to the non-modified nanofluids, as shown in Figure 12. This is mainly due to the presence of SDS and OA compounds in the nanofluids, with both compounds also present as part of the solid fraction in the base oil. This higher viscosity trend indicates that the liquid film thickness of the modified graphene-oil nanofluids is thicker than that of the non-modified ones, which can effectively minimize the direct contact between two sliding surfaces and further reduce friction and wear [44]. Similarly, a trend of decreasing viscosity with increasing temperature was observed for all modified graphene allotropes, with the viscosity of mMWON being the highest, followed by mGNON and mNSON. When compared with heated modified graphene-oil nanofluids, no significant changes in viscosity were observed, as shown in Figure 12.

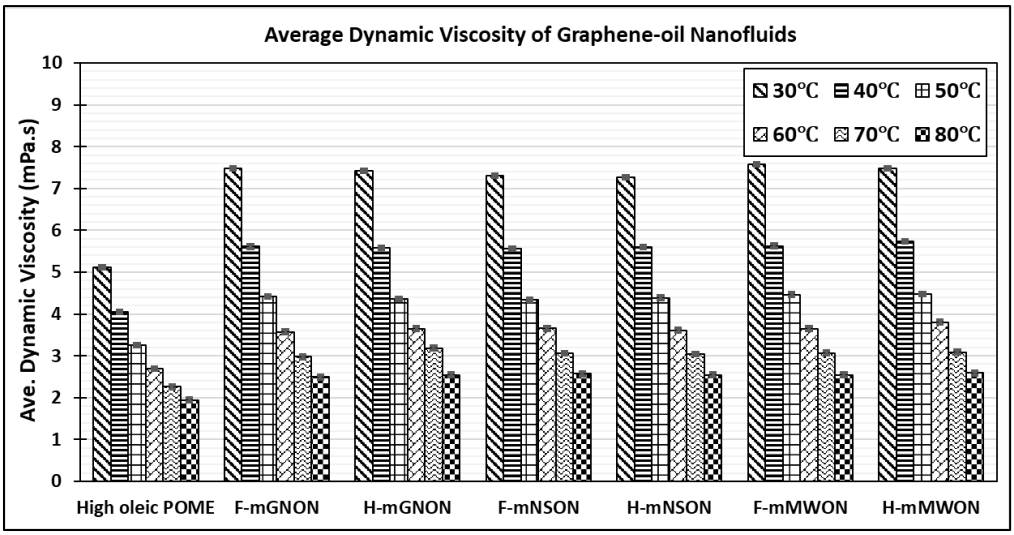

Figure 12. The average dynamic viscosity of fresh and heated modified graphene-oil nanofluids exposed to different temperature ranges from 30 °C to 80 °C (Notes: F = fresh; H = heated).

3.3. Friction and Wear Test Results

Comparing fresh and heated non-modified graphene-oil nanofluids as shown in Figure 13a,c,e, it was found that each graphene oil nanofluid, regardless of whether it is non-heated (fresh) or heated, shows no significant changes in the coefficient of friction (CoF) trend. NSON shows the largest CoF trend reduction, followed by GNON and finally MWON. Inconsistent fluctuations are also observed in the MWON trend, which may be due to the tubular structure of MWCNTs performing various lubrication mechanisms. In addition, MWCNTs may also break off and form sharp fragments, resulting in inconsistent roughness of the lubricating surfaces and contributing to a higher CoF trend. This was later confirmed by the microscopic images of the worn surfaces of the pins in Figure 17c. On the other hand, for GNON and NSON, due to the smaller size of the NSG nanoparticles, NSON tends to slip the NSG nanoparticles into the gap between the asperities more effectively than GNP, which is slightly larger, thus performing the mending mechanism more effectively and bringing significant reduction in friction and wear [16]. This is confirmed in Figure 17b,d by the micrographs of the worn surface of the pin with GNON and NSON lubrication, respectively, where the deep grooves of the pin with NSON lubrication are relatively smaller than those of the pin with GNON lubrication. The highest friction reduction of 52.03% was observed with NSON lubrication compared to plain high oleic POME (average CoF reduction from 0.12 to 0.06). Apart from this, NSON also shows the best reduction in pin weight loss of 59.27% compared to plain high oleic POME (reduction in pin weight loss from 32.9 mg to 13.4 mg). Figure 14 shows the results of pin weight loss reduction by different graphene-oil nanofluids in non-heated (fresh) and heated conditions.

Moreover, no significant changes are observed in the modified graphene-oil nanofluids in terms of CoF trend when comparing the non-heated (fresh) and heated conditions (see Figure 13b,d,f). This time, mGNON shows the best CoF trend reduction, followed by mNSON and, finally, mMWON. The lowest CoF trend is no longer achieved by NSG, as in the case of the non-modified category, which is mainly due to the nature of graphite, which is a compact stacked structure of graphene layers, giving it a relatively small surface area compared to graphene structures [45]. Thus, NSG provides less space for SDS to adhere to the surface of NSG. Similar observations were made in another study in which the authors investigated the adsorption of antibiotics on graphite and graphene structures. Later, it was found that graphene structures have better antibiotic adhesion than graphite structures because the surface area of the graphene layer is larger than that of graphite [46]. Thus, the increase of hydrophobicity in NSG compared to GNP during surface modification by SDS and OA is not significant. The structure of GNP is completely platelet-shaped,

which provides a larger space for the adhesion of SDS on the GNP surface. Since part of SDS cannot adhere to the NSG surface, some parts remain in the solution of NSG–SDS-OA. When dried in the furnace, SDS tends to dry out and form crystallized solids, which lead to higher friction and wear due to abrasion of the third body [47,48] during sliding operations. Figure 15 shows the crystallized SDS observed in mNSON with a 400 mesh filter screen. Inconsistent fluctuations can still be observed in the mMWON trend because the modification of MWCNT does not change the tubular structure of MWCNT or prevent fragments from breaking.

All non-modified and modified graphene-oil nanofluids show a reduction CoF trend compared to pure high oleic POME, which is mainly due to the formation of a self-lubricating graphene tribo-film on the lubricating surfaces [23,49,50]. The best friction and wear reduction was found for mGNON, which exhibits an average CoF reduction of 60.5% compared to pure high oleic POME (average CoF reduction from 0.12 to 0.047). At the same time, as described in Section 3.2, mGNON, with its excellent fluid film thickness, also shows an excellent 99.4% reduction in pin weight loss compared to pure high oleic POME (pin weight loss reduction from 32.9 mg to 0.2 mg). Figure 16 shows the reduction in weight loss of pins by different modified graphene-oil nanofluids in non-heated (fresh) and heated conditions.

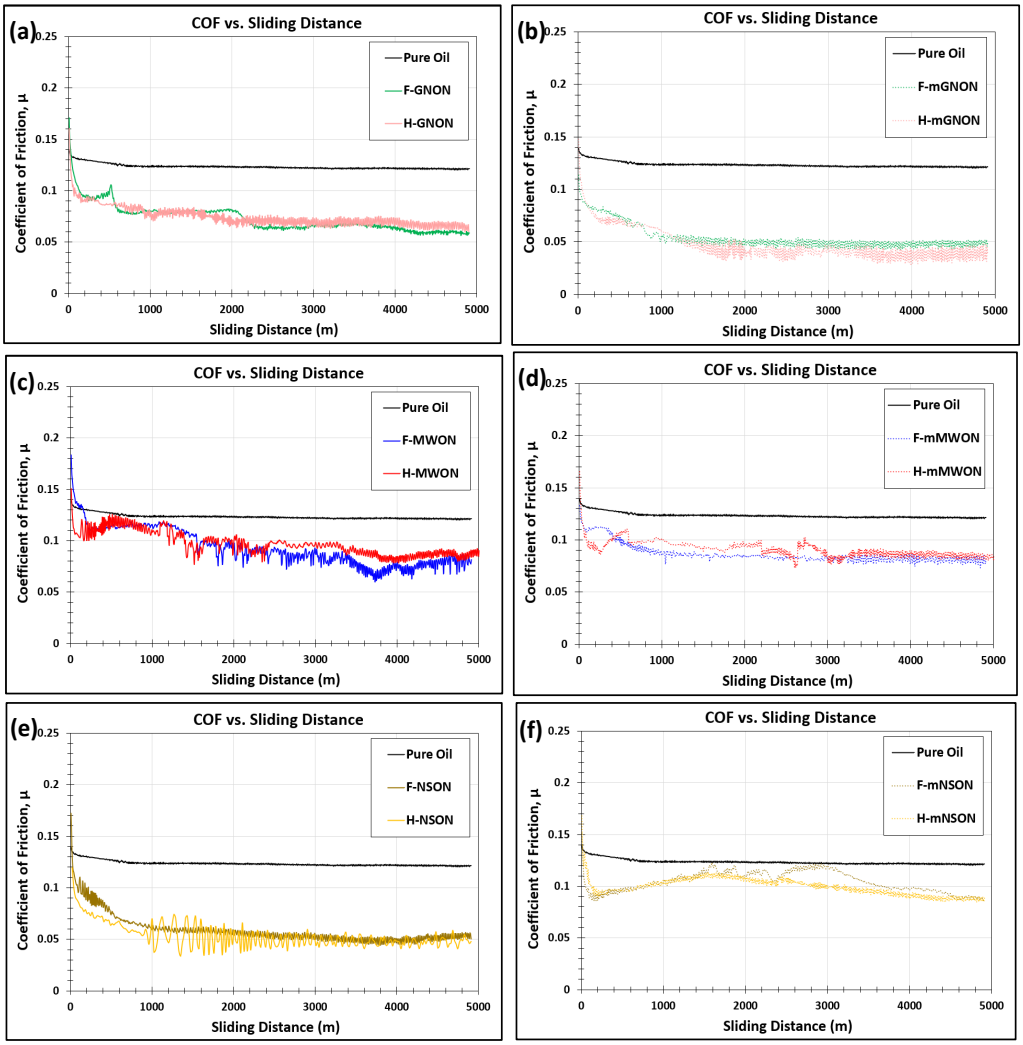

Figure 13. Friction coefficient for non-heated (fresh) and heated (**a**) GNON, (**b**) mGNON, (**c**) MWON, (**d**) mMWON, (**e**) NSON and (**f**) mNSON lubrication as compared to pure oil at constant normal load of 44.15 N and sliding speed of 1.36 m/s for 3600 s (Notes: F = fresh; H = heated).

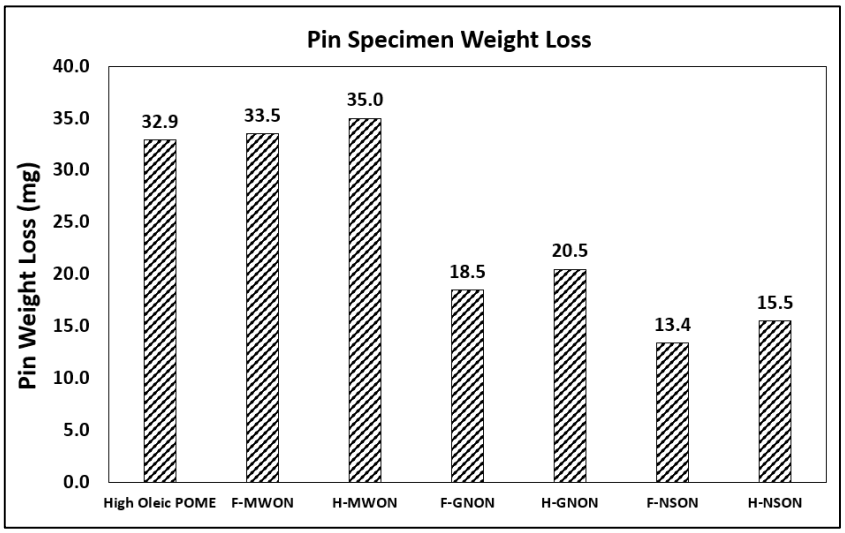

Figure 14. Pin weight loss for non-heated (fresh) and heated graphene-oil nanofluids as compared to high oleic POME at constant normal load of 44.15 N and sliding speed of 1.36 m/s for 3600 s (Notes: F = fresh; H = heated).

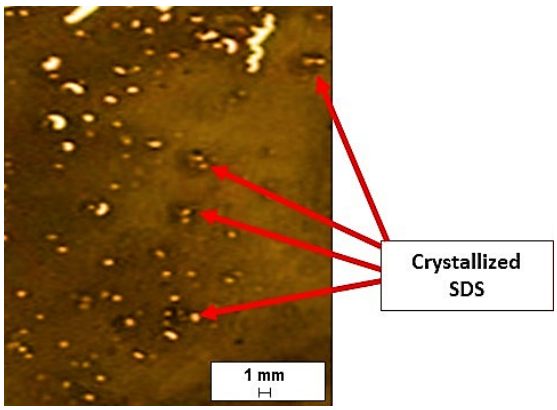

Figure 15. Crystallized SDS formed observed in mNSON after being filtered using 400 mesh filter screen.

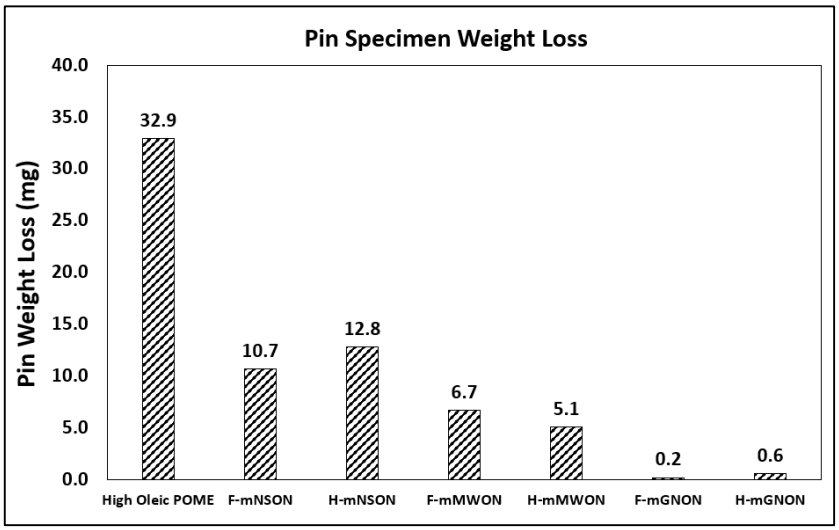

Figure 16. Pin weight loss for fresh and heated modified graphene-oil nanofluids as compared to high oleic POME at constant normal load of 44.15 N and constant sliding speed of 1.36 m/s for 3600 s (Notes: F = fresh; H = heated).

3.4. Pin Worn Surface Micrographs

Figure 17 shows the microscopic images of the worn surface of the pin for heated non-modified graphene-oil nanofluid lubrications, while Figure 18 shows microscopic images of the worn surface of the pin for heated modified graphene-oil nanofluid lubrications. Fewer scratches and grooves are observed in the modified graphene-oil nanofluid lubricated pin specimens, which can be attributed to the thicker fluid film thickness due to the higher dynamic viscosity of the modified graphene-oil nanofluid. This thicker fluid film thickness helps to minimize the probability of direct contact between the pin and the ring during the lubrication process [44].

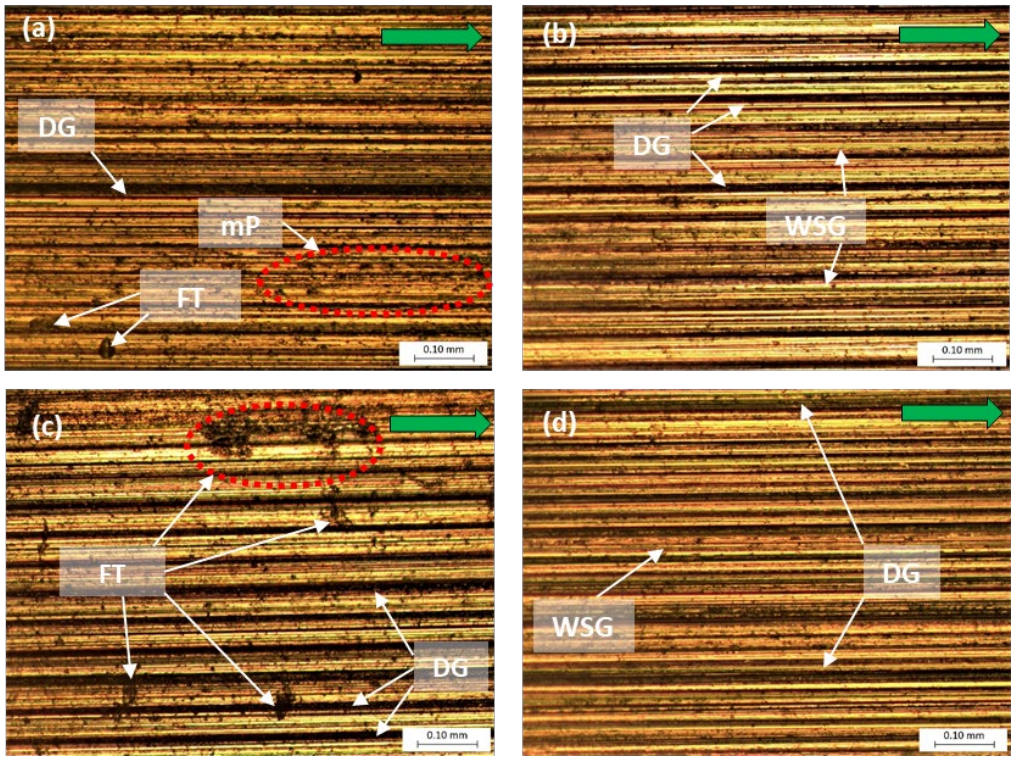

Figure 17. Micrographs of pin specimen worn surfaces tested with (**a**) high oleic POME, (**b**) GNON, (**c**) MWON and (**d**) NSON lubrication at constant normal load of 44.15 N and constant sliding speed of 1.36 m/s for 3600 s under 10× magnification (Notes: Green arrow = sliding direction; DG = deep groove; mP = micro-pits; WSG = wide-shallow groove; FT = fracture).

It can be observed that the worn surfaces of the pins in MWON lubrication in Figure 17c have several areas of pitting and severe scratches, which are mainly due to the scratching of MWCNT agglomerations formed after the sonication process [43]. Since modified MWCNTs in mMWON still tend to break off and form sharp fragments, some deep grooves can be observed on the worn surface of the pin (see Figure 18c), but they are not as pronounced as those on the non-modified one in Figure 17c due to the effective thickness of the fluid film in mMWON [44]. Some deep grooves can also be observed on the worn surface of the pin in mNSON lubrication (see Figure 18d), which is mainly due to the crystallized SDS in mNSON.

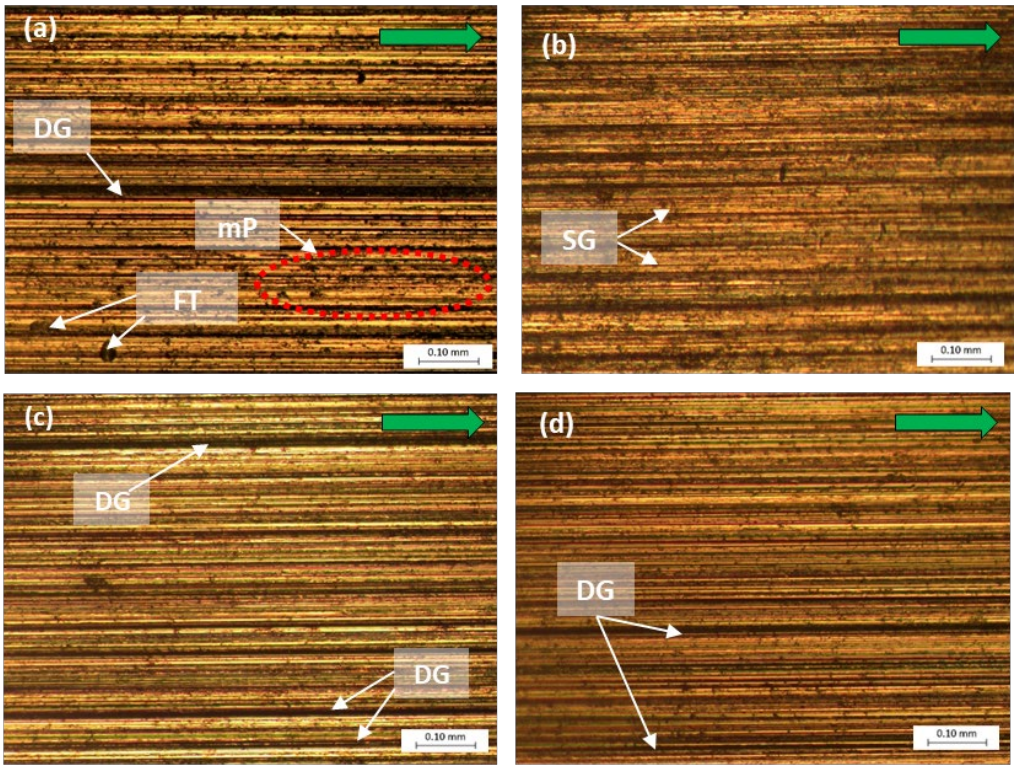

Figure 18. Micrographs of pin specimen worn surfaces tested with (**a**) high oleic POME, (**b**) mGNON, (**c**) mMWON and (**d**) mNSON lubrication at constant normal load of 44.15 N and constant sliding speed of 1.36 m/s for 3600 s under 101× magnification (Notes: Green arrow = sliding direction; DG = deep groove; mP = micro-pits; SG = shallow groove; FT = fracture).

4. Conclusions

This work proves that the synthesized graphene-oil nanofluids can significantly reduce friction and wear compared to pure base oil. Moreover, the modified graphene-oil nanofluids with excellent dispersion stability further reduce friction and wear in contact pairs. In addition, modified graphene-oil nanofluids with better dynamic viscosity have improved the wear resistance of sliding surfaces. mGNON shows an average friction reduction of 60.5% and a 99.4% reduction in the weight loss of pins.

Furthermore, the heated and non-heated synthesized (non-modified and modified) graphene-oil nanofluids show no drastic changes in dynamic viscosity, friction and wear performance. This proves that the thermophysical and tribological properties of graphene-oil nanofluids are not affected when they are heated and cooled back to room temperature. This suggests that the synthesized graphene-oil nanofluids have a longer lifetime and can be used in journal bearings applications without the need for frequent replacement.

Author Contributions: Conceptualization, K.W.L. and K.P.N.; methodology, K.W.L., K.P.N. and E.L.; formal analysis, K.W.L. and K.P.N.; investigation, K.P.N., K.W.L. and E.L.; resources, K.W.L. and E.L.; writing—original draft preparation, K.W.L. and K.P.N.; writing—review and editing, K.W.L., E.L. and K.P.N.; supervision, K.W.L. and E.L.; funding acquisition, E.L. and K.W.L. All authors have read and agreed to the published version of the manuscript.

Funding: This research was funded by Fundamental Research Grant Scheme (FRGS/1/2019/TK03/MMU/03/3).

Data Availability Statement: Available upon request.

Acknowledgments: This work was supported by Fundamental Research Grant Scheme (FRGS), Ministry of Higher Education, Malaysia. Special thanks to the Faculty of Engineering and Technology of Multimedia University, Malaysia for their support in allowing this research to be carried out.

Conflicts of Interest: The authors declare no conflict of interest.

References

1. Cameron, A.; Wood, W.L. The full journal bearing. *Proc. Inst. Mech. Eng.* **1949**, *161*, 59–72. [CrossRef]
2. Ünlü, B.S.; Atik, E. Determination of friction coefficient in journal bearings. *Mater. Des.* **2007**, *28*, 973–977. [CrossRef]
3. Litwin, W. Marine propeller shaft bearings under low-speed conditions: Water vs. oil lubrication. *Tribol. Trans.* **2019**, *62*, 839–849. [CrossRef]
4. de Azevedo, H.D.; Araújo, A.M.; Bouchonneau, N. A review of wind turbine bearing condition monitoring: State of the art and Challenges. *Renew. Sustain. Energy Rev.* **2016**, *56*, 368–379. [CrossRef]
5. Dutta, S. Positive Outlook for Wind-Turbine Lubricants. 2019. Available online: https://www.windpowerengineering.com/positive-outlook-for-wind-turbine-lubricants/ (accessed on 21 August 2022).
6. Feng, Y.; Qiu, Y.; Crabtree, C.J.; Long, H.; Tavner, P.J. Monitoring wind turbine gearboxes. *Wind Energy* **2012**, *16*, 728–740. [CrossRef]
7. Hennigan, G.; Page, C. Maximizing Maintenance Dollars In a Post-PTC World. 2018. Available online: https://www.mobil.com/en/industrial/~{}/media/7EDB938B727C4B59B7BE32EE8DB82053.ashx (accessed on 21 August 2022).
8. Moghadam, A.D.; Omrani, E.; Menezes, P.L.; Rohatgi, P.K. Mechanical and tribological properties of self-lubricating metal matrix nanocomposites reinforced by carbon nanotubes (CNTs) and graphene—A review. *Compos. Part B Eng.* **2015**, *77*, 402–420. [CrossRef]
9. Tevrüz, T. Tribological behaviours of carbon filled polytetrafluoroethylene (PTFE) dry journal bearings. *Wear* **1998**, *221*, 61–68. [CrossRef]
10. Kim, S.S.; Park, D.C.; Lee, D.G. Characteristics of carbon fiber phenolic composite for journal bearing materials. *Compos. Struct.* **2004**, *66*, 359–366. [CrossRef]
11. Srivyas, P.D.; Charoo, M.S. Friction and wear reduction by graphene nano platelets for hybrid nano aluminium matrix composite under dry sliding conditions. *Metall. Mater. Eng.* **2020**, *27*, 27–47. [CrossRef]
12. Zhang, G.; Xu, Y.; Xiang, X.; Zheng, G.; Zeng, X.; Li, Z.; Ren, T.; Zhang, Y. Tribological performances of highly dispersed graphene oxide derivatives in vegetable oil. *Tribol. Int.* **2018**, *126*, 39–48. [CrossRef]
13. Song, H.; Wang, Z.; Yang, J. Tribological properties of graphene oxide and carbon spheres as lubricating additives. *Appl. Phys. A* **2016**, *122*, 933. [CrossRef]
14. Senatore, A.; D'Agostino, V.; Petrone, V.; Ciambelli, P.; Sarno, M. Graphene oxide nanosheets as effective friction modifier for oil lubricant: Materials, methods, and tribological results. *ISRN Tribol.* **2013**, *2013*, 425809. [CrossRef]
15. Chengara, A.; Nikolov, A.D.; Wasan, D.T.; Trokhymchuk, A.; Henderson, D. Spreading of nanofluids driven by the structural disjoining pressure gradient. *J. Colloid Interface Sci.* **2004**, *280*, 192–201. [CrossRef] [PubMed]
16. Singh, R.K.; Dixit, A.R.; Sharma, A.K.; Tiwari, A.K.; Mandal, V.; Pramanik, A. Influence of graphene and multi-walled carbon nanotube additives on tribological behaviour of lubricants. *Int. J. Surf. Sci. Eng.* **2018**, *12*, 207–227. [CrossRef]
17. Fillon, M.; Bouyer, J. Thermohydrodynamic analysis of a worn plain journal bearing. *Tribol. Int.* **2004**, *37*, 129–136. [CrossRef]
18. Yunus, M.; Munshi, S.M. Performance Evaluation of Hydrodynamic Journal Bearing using Gearbox and Engine Oil (SAE90 and SAE20w50) by Experimental and Theoretical Methods. *Int. J. Mech. Eng. Inf. Technol.* **2015**, *3*, 1573–1583.
19. Bao, T.; Wang, Z.; Zhao, Y.; Wang, Y.; Yi, X. Long-term stably dispersed functionalized graphene oxide as an oil additive. *RSC Adv.* **2019**, *9*, 39230–39241. [CrossRef]
20. Lin, J.; Wang, L.; Chen, G. Modification of graphene platelets and their tribological properties as a lubricant additive. *Tribol. Lett.* **2010**, *41*, 209–215. [CrossRef]
21. Soudagar, M.E.; Nik-Ghazali, N.-N.; Kalam, M.A.; Badruddin, I.A.; Banapurmath, N.R.; Khan, T.M.Y.; Bashir, M.N.; Akram, N.; Farade, R.; Afzal, A. The effects of graphene oxide nanoparticle additive stably dispersed in dairy scum oil biodiesel-diesel fuel blend on CI engine: Performance, emission and combustion characteristics. *Fuel* **2019**, *257*, 116015–116031. [CrossRef]
22. Tummala, N.R.; Grady, B.P.; Striolo, A. Lateral confinement effects on the structural properties of surfactant aggregates: SDS on graphene. *Phys. Chem. Chem. Phys.* **2010**, *12*, 13137–13143. [CrossRef]
23. La, D.D.; Truong, T.N.; Pham, T.Q.; Vo, H.T.; Tran, N.T.; Nguyen, T.A.; Nadda, A.K.; Nguyen, T.T.; Chang, S.W.; Chung, W.J.; et al. Scalable fabrication of modified graphene nanoplatelets as an effective additive for engine lubricant oil. *Nanomaterials* **2020**, *10*, 877. [CrossRef]
24. Aleklett, K.; Höök, M.; Jakobsson, K.; Lardelli, M.; Snowden, S.; Söderbergh, B. The peak of the oil age—Analyzing the world oil production reference scenario in World Energy Outlook 2008. *Energy Policy* **2010**, *38*, 1398–1414. [CrossRef]
25. Mobarak, H.M.; Mohamad, E.N.; Masjuki, H.H.; Kalam, M.A.; al Mahmud, K.A.H.; Habibullah, M.; Ashraful, A.M. The prospects of biolubricants as alternatives in automotive applications. *Renew. Sustain. Energy Rev.* **2014**, *33*, 34–43. [CrossRef]
26. Udonne, J.D. A comparative study of recycling of used lubrication oils using distillation, acid and activated charcoal with clay methods. *J. Pet. Gas Eng.* **2011**, *2*, 12–19.
27. Naddaf, A.; Heris, S.Z.; Pouladi, B. An experimental study on heat transfer performance and pressure drop of nanofluids using graphene and multi-walled carbon nanotubes based on diesel oil. *Powder Technol.* **2019**, *352*, 369–380. [CrossRef]
28. McCash, L.B.; Akhtar, S.; Nadeem, S.; Saleem, S. Entropy analysis of the peristaltic flow of hybrid nanofluid inside an elliptic duct with sinusoidally advancing boundaries. *Entropy* **2021**, *23*, 732. [CrossRef]

29. Ali, A.; Saleem, S.; Mumraiz, S.; Saleem, A.; Awais, M.; Marwat, D.N.K. Investigation on tio2–cu/H2O hybrid nanofluid with slip conditions in MHD peristaltic flow of Jeffrey Material. *J. Therm. Anal. Calorim.* **2020**, *143*, 1985–1996. [CrossRef]
30. Berman, D.; Erdemir, A.; Sumant, A.V. Graphene: A new emerging lubricant. *Mater. Today* **2014**, *17*, 31–42. [CrossRef]
31. Li, Q.; Lee, C.; Carpick, R.W.; Hone, J. Substrate effect on thickness-dependent friction on graphene. *Phys. Status Solidi (B)* **2010**, *247*, 2909–2914. [CrossRef]
32. Davis, J.R. *Alloying: Understanding the Basics*; ASM International: Materials Park, OH, USA, 2011.
33. Meyer, T. Validation of Journal Bearings for Use in Wind Turbine Gearboxes. 2015. Available online: https://www.windsystemsmag.com/educational-opportunities-abound-at-windpower-2015/ (accessed on 21 August 2022).
34. Pantazopoulos, G.; Papaefthymiou, S. Failure and fracture analysis of austenitic stainless steel marine propeller shaft. *J. Fail. Anal. Prev.* **2015**, *15*, 762–767. [CrossRef]
35. Lorenzi, S.; Pastore, T.; Bellezze, T.; Fratesi, R. Cathodic protection modelling of a propeller shaft. *Corros. Sci.* **2016**, *108*, 36–46. [CrossRef]
36. Hantoro, R.H.; Utama, I.K.; Sulisetyono, A.S.; Erwandi, E. Validation of lumped mass lateral cantilever shaft vibration simulation on fixed-pitch vertical-axis ocean current turbine. *IPTEK J. Technol. Sci.* **2010**, *21*, 1–8. [CrossRef]
37. Kanwal, S.; Ali, N.Z.; Hussain, R.; Shah, F.U.; Akhter, Z. Poly-thiourea formaldehyde based anticorrosion marine coatings on type 304 stainless steel. *J. Mater. Res. Technol.* **2020**, *9*, 2146–2153. [CrossRef]
38. Jayadas, N.H.; Nair, K.P. Coconut oil as base oil for industrial lubricants—evaluation and modification of thermal, oxidative and low temperature properties. *Tribol. Int.* **2006**, *39*, 873–878. [CrossRef]
39. Bhushan, B. *Introduction to Tribology*; Wiley: New York, OH, USA, 2013.
40. Ng, K.P.; Liew, K.W.; Lim, E. Role of eco-friendly bio-based graphene-oil nanofluids on friction reduction for wind turbine application. In Proceedings of the IOP Conference Series: Earth and Environmental Science, Sapporo, Japan, 26–28 August 2021; p. 012012.
41. Krisnangkura, K.; Yimsuwan, T.; Pairintra, R. An empirical approach in predicting biodiesel viscosity at various temperatures. *Fuel* **2006**, *85*, 107–113. [CrossRef]
42. Konijn, B.J.; Sanderink, O.B.J.; Kruyt, N.P. Experimental study of the viscosity of suspensions: Effect of solid fraction, particle size and suspending liquid. *Powder Technol.* **2014**, *266*, 61–69. [CrossRef]
43. Zhang, L.; Pu, J.; Wang, L.; Xue, Q. Frictional dependence of graphene and carbon nanotube in diamond-like carbon/ionic liquids hybrid films in vacuum. *Carbon* **2014**, *80*, 734–745. [CrossRef]
44. Fang, Y.; Ma, L.; Luo, J. Modelling for water-based liquid lubrication with ultra-low friction coefficient in rough surface point contact. *Tribol. Int.* **2020**, *141*, 105901–105908. [CrossRef]
45. Ferrer, P.R.; Mace, A.; Thomas, S.N.; Jeon, J.-W. Nanostructured porous graphene and its composites for energy storage applications. *Nano Converg.* **2017**, *4*, 29. [CrossRef]
46. Carrales-Alvarado, D.H.; Rodríguez-Ramos, I.; Leyva-Ramos, R.; Mendoza-Mendoza, E.; Villela-Martínez, D.E. Effect of surface area and physical–chemical properties of graphite and graphene-based materials on their adsorption capacity towards metronidazole and trimethoprim antibiotics in aqueous solution. *Chem. Eng. J.* **2020**, *402*, 126155. [CrossRef]
47. Abdelbary, A. Sliding mechanics of polymers. In *Wear of Polymers and Composites*; Woodhead Publishing: Thorston, UK, 2014; pp. 37–66.
48. Halim, T.; Burgett, M.; Donaldson, T.K.; Savisaar, C.; Bowsher, J.; Clarke, I.C. Profiling the third-body wear damage produced in cocr surfaces by bone cement, COCR, and ti6al4v debris: A 10-cycle metal-on-metal simulator test. *Proc. Inst. Mech. Eng. Part H J. Eng. Med.* **2014**, *228*, 703–713. [CrossRef] [PubMed]
49. Rasheed, A.K.; Khalid, M.; Rashmi, W.; Gupta, T.C.S.M.; Chan, A. Graphene based nanofluids and nanolubricants—Review of recent developments. *Renew. Sustain. Energy Rev.* **2016**, *63*, 346–362. [CrossRef]
50. Tjong, S.C. Recent progress in the development and properties of novel metal matrix nanocomposites reinforced with carbon nanotubes and graphene nanosheets. *Mater. Sci. Eng. R Rep.* **2013**, *74*, 281–350. [CrossRef]